

A Quantum Mechanical Investigation of the Nature of the Dative Bond in Crystalline 1-Chlorosilatrane

Jan Dillen[†]

Department of Chemistry, University of Stellenbosch, Private Bag XI, Matieland 7602, South Africa

Received: February 25, 2004; In Final Form: April 1, 2004

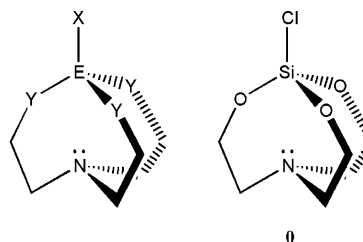
The molecular geometry of crystalline 1-chlorosilatrane is computed at the self-consistent field (SCF) and density functional theory (DFT) levels of theory with the 6-31G* basis set and compared with experiment. The calculations reproduce the shortening of the Si–N distance in the crystal relative to the gas phase, in agreement with existing experimental data for methyl- and fluorosilatrane. The bond shortening is shown to be the result of a combination of a conformational change in the molecule and dipole–dipole interactions with the surrounding molecules in the crystal. The importance of the need to include long-range interactions in the calculation is demonstrated. The calculated electron density of chlorosilatrane is analyzed in terms of the natural bond orbital formalism (NBO), natural resonance theory (NRT), and the theory of atoms in molecules (AIM).

Introduction

Silatrane is a biologically active compound whose pharmacodynamical properties were reviewed about 25 years ago.¹ Historically, silatrane was the first example of a structure of the form given in Chart 1, now generally referred to as “atranes”, with E = Si and Y = O.

The chemical and structural features of main group atranes, including silatrane, have been reviewed by Verkade.² From a topological point of view, silatrane can exist in two different forms. In the exo form, the lone pair of the nitrogen atom is directed outward from the cage, thus potentially allowing coordination with a Lewis acid. In the endo variety, the lone pair is directed inward toward the silicon atom, creating the possibility of a transannular Si–N bond. A survey of 95 crystalline silatrane derivatives in the current (5.24) version of the Cambridge Structural Database³ shows that, after elimination of four entries with X = Os, the average Si–N distance is equal to 2.14(7) Å and the X–Si–O valence angle 96(3)°, both indicative of an existing bonding interaction between Si and N, and thus a pentacoordinated Si atom. This is in sharp contrast to the information obtained from gas phase electron diffraction data (GED). Shen and Hilderbrandt⁴ determined the structure of methylsilatrane and found a Si–N distance of 2.45(5) Å, indicating that there essentially is no dative bond between the Si and N atoms. In the crystalline state,⁵ this value is found to be 2.175(4) Å. In another study, Hargittai et al.⁶ also used GED to study fluorosilatrane. They found a Si–N distance of 2.324(14) Å, compared to a value of 2.042(1) in the crystal.⁷ In the latter study, experimental charge density maps revealed the existence of increased electron density between the Si and N atoms. On the basis of the linear relationship that was found between the nonplanarity of the Si atom and the value of the Si–N distance as found in the crystalline state, Greenberg et al.^{8a} have questioned the notion that there is no dative bond between Si and N in the gas phase, as the data for the isolated molecule are within reasonable agreement with the trend observed for the solid state.

CHART 1: Schematic Drawing of the General Structure of Atranans (Left), and of 1-Chlorosilatrane in Particular (Right)



1-Substituted silatrane derivatives have also attracted considerable computational interest. Greenberg et al.^{8b} performed single point Hartree–Fock (HF) calculations on two bond stretch isomers of methylsilatrane and found little difference in the charge distributions of the two forms when using the 3-21G* basis set. Gordon and co-workers⁹ performed a HF/6-31G* calculation on AM1-optimized geometries of silatrane and concluded that about 26 kJ/mol is required to shorten the Si–N bond from the length found in the gas phase to that of the crystal, suggesting that crystal forces are responsible for the observed shortening. They also reported the existence of a bond critical point¹⁰ between the Si and N atoms and concluded from the calculated properties of the electron density and its second derivative that the bond between the two atoms is a closed shell interaction. Csonka and Hencsei^{11–13} used MNDO, AM1, and PM3 to calculate the equilibrium geometries of 1-fluoro, 1-methyl, and 1-chlorosilatrane, and concluded that both the endo- and exo-forms are energy minima. A further study¹⁴ on fluorosilatrane employing full geometry optimization at the HF level and the 3-21G, 3-21G* and 6-31G* basis sets showed that the previously predicted existence of a stable exo form is an artifact of the semiempirical calculations. Moreover, they also found that the silatrane skeleton is very flexible and that only a small amount of energy is required to shorten the transannular Si–N distance.

Boggs et al.¹⁵ used HF/6-311G* and MP2/6-31G energies of MNDO geometries of methyl- and fluorosilatrane to confirm that there is no stable exo conformation but a broad potential

[†] E-mail address: jldm@sun.ac.za.

energy function with a single maximum at one Si–N distance. They also found that Møller–Plesset (MP2) electron correlation has a sizable influence on the calculated results with the Si–N bond being about 0.15 Å shorter with MP2 compared to HF. Dahl and Skancke¹⁶ used HF/3-21G* with full geometry optimization to conclude the existence of a weak transannular interaction in fluoro-, methyl-, and the parent silatrane. Csonka and Hencsei^{17,18} repeated some of their calculations with various basis sets at the SCF, MP2, and DFT levels of theory, confirming the low energy requirements to shorten the Si–N distance. They also performed self-consistent reaction field (SCRf) calculations using the Onsager model¹⁹ reporting a shortening of the Si–N interaction for the chloro- and fluoro-silatrane. Chung et al.²⁰ studied isothiocyanosilatrane at the SCF and DFT levels of theory with the 6-31+G* and the 6-311G* basis sets. They calculated that the Si–N bond is shorter when calculated with B3LYP as compared to SCF, whereas the Si–O bond is longer. They also looked at the atomic charges calculated with natural population analysis²¹ and found little difference of the charge of the nitrogen atom as a function of substituents. Finally, in a comprehensive study on the inductive effects in pentacoordinated silicon compounds containing a Si←N dative bond, Anglada et al.²² performed MP2 and B3LYP calculations on fluoro- and methylsilatranes, among many other compounds, to conclude that the Si–N bond gets shorter as the number of electron withdrawing groups linked to the silicon atoms increases.

Noticeable differences between the gas phase and solid state value of the length of donor–acceptor bonds are of course not limited to silatranes. For example, a large amount of experimental data is available for complexes containing the B–N dative bond. A review of these and other complexes is given by Haaland.²³ A theoretical explanation of this phenomenon was proposed by Schleyer et al.²⁴ Using SCRf calculations on BH₃NH₃, they calculated that with hexane as a solvent, the B–N bond reduces from 1.689 Å for the isolated molecule to 1.62 Å in solution. In water, the value reduces to 1.57 Å. On the basis of these results, they proposed that the crystal field is responsible for the observed shortening. In another ab initio study,²⁵ Frenking et al. used a dimer and tetramer model of the same molecule to simulate the solid state and concluded that short-range dipole–dipole interactions are causing this effect. Using clusters of BH₃NH₃ molecules of increasing size, Dillen and Verhoeven²⁶ have shown that the addition of molecules to the cluster with stabilizing dipole–dipole interactions decreases the length of the B–N bond whereas destabilizing interactions have the opposite influence. It was also shown that the effect is felt over a large distance between the interacting molecules, thus highlighting the long-range and, hence, electrostatic nature of the interaction.

This paper is the second in a series to study the effect of the crystalline state on the nature of the dative bond by means of ab initio calculations. Although no experimental gas phase structure has been reported to make a comparison possible with the crystal, 1-chlorosilatrane was chosen because of its high symmetry in the solid state and hence its (relative) computational efficiency. In particular, the existence or nonexistence of a “bonding” interaction between the Si and N atoms is investigated.

Computational Details

Calculations were performed with the Gaussian 98 program²⁷ at the self-consistent field (SCF) level of theory and the standard 6-31G* basis set. A few calculations were also performed with

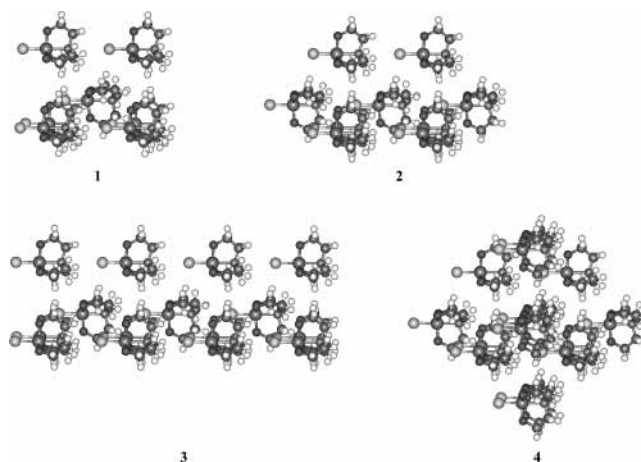
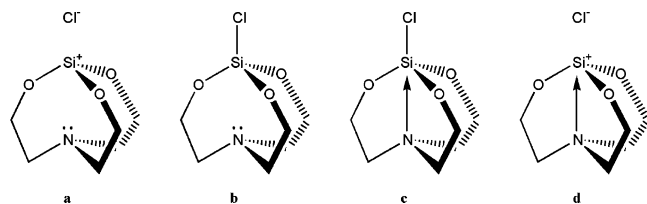


Figure 1. Computational models used to simulate the crystalline state. Position and geometry of the central molecule is allowed to change. Positions of the surrounding molecules are fixed. See text for details.

density functional theory (DFT) using the B3LYP functional and the same basis set as above.

A potential energy surface of the isolated molecule was calculated with the N–Si–C–O and O–Si–N–C torsion angles as fixed grid variables while optimizing all other internal degrees of freedom. It was also assumed that three rings in the silatrane molecule change their conformation in a concerted fashion, keeping overall C₃ symmetry. This restriction is reasonable in view of the symmetry observed in the crystal of chlorosilatrane, and also in the experimental gas phase structures of methyl- and fluorosilatrane.

The crystal environment of chlorosilatrane was simulated by surrounding one molecule with several neighbors, as shown in Figure 1. Coordinates for the surrounding molecules were generated from the experimental X-ray diffraction data of Kemme et al.²⁸ In this paper, the crystal structure was solved and refined in space group *P*2₁, but the data deviate very little from the higher symmetrical space group *P*6₃, the experimental unit cell dimension being $a = 8.176(6)$ Å, $b = 8.176(8)$ Å, $c = 7.951(5)$ Å, and $\beta = 120.01(5)^\circ$. Therefore, mainly to improve computational efficiency, the unit cell and atom coordinates were symmetrized to the higher space group. In addition, the positions of the hydrogen atoms were readjusted by an energy minimization with the UFF force field²⁹ as provided in the Cerius² modeling system,³⁰ while keeping the heavy atoms on their experimental positions. After these modifications, the positions and geometries of the surrounding molecules were fixed during all Gaussian calculations. Both the internal geometry and the position of the central molecule in the cluster were allowed to vary under the constraint that the whole cluster had to keep C₃ symmetry. Four different clusters were studied. In cluster **1**, the central molecule is surrounded by six neighbors, all pointing in the same direction. The Si–N bond of the central molecule is along the C₃ axis. In **2**, two additional molecules are placed along the symmetry axis, bringing the total number of molecules to nine. In terms of dipole–dipole interactions, these two molecules add a stabilizing effect to the central molecule. Model **3** adds an additional six molecules to **2**, all placed along the general direction of the symmetry axis. These add a significant amount of computational effort to the system, increasing the number of basis functions from 1908 to 3180. Again, in terms of classical dipole–dipole interactions, the effect on the central molecule is stabilization. In contrast, model **4**, which adds the same number of molecules to **2**, represents destabilization because parallel dipoles are added alongside the central mol-

CHART 2: Four Lewis Structures Considered as References for the NBO and NRT Analysis


ecule. Ideally, an infinitely large cluster of molecules should be chosen to represent the crystal state. However, because all the different models above all have relatively close neighboring molecules, it is possible to test whether the results can be interpreted in terms of dipole–dipole interactions.

Calculation of vibrational frequencies with the 6-31G(d) basis set proved to be impossible with Gaussian 98 running on 32 bit computer technology even for the smallest cluster **1**. Therefore, the more modest 3-21G* basis set was used, and even then only cluster **1** proved to be within reach. Normal modes on the isolated molecule and cluster **1** were analyzed visually using a vibrational animation program.³¹

ONIOM (Our own *n*-layered integrated molecular orbital and molecular mechanics)³² calculations were done using the Gaussian 98 implementation of the UFF force field, with no charges on the atoms in the outer molecular mechanics layer which consisted of all the molecules in the cluster except the central molecule. The latter formed the inner SCF layer.

Analysis of the electron density in terms of the atoms in molecules (AIM) theory¹⁰ was performed with the AIMPAC suite of computer programs as supplied by Bader's research group. The programs were modified to handle larger systems, but were otherwise used unaltered.

Natural bond orbital³³ (NBO) analysis was done with the NBO 5.0 computer program,³⁴ incorporated as a "link" into the Gaussian 98 program, as explained in the program manual.

Finally, a natural resonance theory³⁵ (NRT) analysis was performed on the isolated molecule. In a first series of calculations, each of the Lewis structures **a–d** (see Chart 2) was used in a single-reference NRT analysis, which implies that there is one dominant resonance structure. In a second series, the combinations **a+b**, **b+c**, and **b+d** were used in a multi-reference analysis.

Results and Discussion

Before investigating the effect of the solid state on the nature of the Si–N bonding interaction, it is worthwhile to look at any "internal" means to change the Si–N distance in the chlorosilatrane molecule. As mentioned before, several computational studies have indicated^{9,14,15,17,18} that little energy is required to shorten the Si–N distance from its value calculated for the isolated molecule to the value found in the crystal, and that the silatrane skeleton is very flexible. The calculations indicate that in the gas phase, the five-membered ring formed by the atoms Si–O–C–C–N is considerably more puckered than in the crystal. There is also a difference in conformation. In the isolated molecule, the five-membered rings adopt an envelope conformation with the carbon atom adjacent to the oxygen forming the "tip", whereas in the crystal, a twist conformation is found with the pseudo 2-fold axis passing through the silicon atom and the C–C bond. Both forms are adjacent conformations on the pseudorotational pathway of the five-membered ring. To study the already mentioned flexibility of the silatrane skeleton, a potential energy surface was

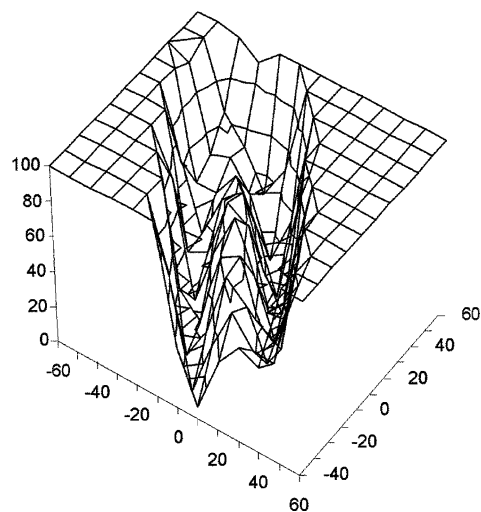


Figure 2. Conformational potential energy surface of chlorosilatrane as a function of the N–Si–C–O (right axis) and O–Si–N–C (left axis) torsion angles. Energies (kJ/mol, vertical axis) are relative to the most stable conformation.

calculated as a function of the N–Si–C–O and O–Si–N–C torsion angles, as explained earlier. A diagram of the resulting two-dimensional energy map, calculated with a 10° grid size, is shown in Figure 2.

It can be seen that the chlorosilatrane molecule can adopt several conformations that are within a 20–25 kJ/mol reach of the single most stable form. This "valley" of low energy corresponds to the pseudorotational motion of the five-membered rings. A second area of low energy corresponds to all five-membered rings being inverted and is thus related by symmetry to the first one. The lowest energy barrier between the two valleys is about 55 kJ/mol. Although no disorder is reported for the crystal structure of chlorosilatrane,²⁸ the size of the temperature factors indicates very high thermal movement of the carbon atoms adjacent to the nitrogen atom. Structural disorder is mentioned for both the crystal structures of methylsilatrane⁵ and fluorosilatrane.⁷ Hence, it appears reasonable to assume that the conformational flexibility of the silatrane molecule is responsible for this phenomenon. Important for the current discussion, however, is the fact that during these conformational changes, the value of the Si–N distance can vary quite considerably. Hence, before starting a full quantum mechanical calculation of clusters **1–4**, an ONIOM calculation was performed to investigate the effect of crystal packing on the conformation of the silatrane molecule and the Si–N bond length. Although the details of the results for the four calculations differ slightly, they are similar enough to concentrate on one set of data, which is given in Table 1. Results for all ONIOM calculations are given in the Supporting Information. Most noticeable is the shortening of the Si–N distance in the crystal by ~0.2 Å compared to the isolated molecule. The five-membered rings also change conformation from an envelope to a twist form, as found experimentally. However, the overall puckering of the ring is calculated to be too high. The change in conformation also triggers changes in the individual valence angles. The Cl–Si–O and O–Si–N angles, both indicators of a change from a tetrahedral arrangement around Si to a trigonal bipyramid, change toward the experimental values observed in the crystal. The Si–O–C angle also increases whereas the opposite is found experimentally. Because no charges were assigned to the atoms in the molecular mechanics layer of the ONIOM calculations, only the van der Waals interactions are responsible for the observed changes.

TABLE 1: Calculated (HF/6-31G*) and Experimental Data for 1-Chlorosilatrane^a

| model | gas | | | Xtal | | | |
|---|---------|---------|---------|---------|---------|---------|------------------------------------|
| | 0 | 1 | 2 | 3 | 4 | ONIOM 3 | exp ^b (C ₃) |
| Si-N | 2.571 | 2.260 | 2.130 | 2.073 | 2.379 | 2.370 | 2.023 |
| Cl-Si | 2.058 | 2.075 | 2.098 | 2.129 | 2.041 | 2.062 | 2.153 |
| Si-O | 1.633 | 1.648 | 1.653 | 1.654 | 1.641 | 1.639 | 1.649 |
| O-C | 1.401 | 1.400 | 1.401 | 1.405 | 1.392 | 1.392 | 1.416 |
| C-C | 1.527 | 1.524 | 1.521 | 1.521 | 1.523 | 1.526 | 1.435 |
| C-N | 1.449 | 1.457 | 1.467 | 1.471 | 1.452 | 1.454 | 1.449 |
| Cl-Si-O | 104.4 | 98.6 | 95.9 | 94.5 | 100.7 | 100.5 | 93.3 |
| Si-O-C | 124.6 | 125.6 | 123.3 | 121.9 | 127.0 | 127.2 | 120.2 |
| O-C-C | 109.8 | 108.9 | 108.4 | 108.3 | 109.7 | 109.9 | 111.1 |
| C-C-N | 108.8 | 107.7 | 107.2 | 106.9 | 108.1 | 108.1 | 111.6 |
| O-Si-N | 76.0 | 81.4 | 84.1 | 84.5 | 79.3 | 79.5 | 86.7 |
| Si-N-C | 98.5 | 103.0 | 104.3 | 104.9 | 101.2 | 101.5 | 105.9 |
| O-Si-O | 114.4 | 117.8 | 119.0 | 119.4 | 116.6 | 116.8 | 119.7 |
| C-N-C | 117.9 | 115.1 | 114.1 | 113.6 | 116.3 | 116.1 | 112.8 |
| O-Si-N-C | -0.3 | -14.3 | -15.8 | -16.3 | -11.8 | -12.0 | -9.2 |
| C-O-Si-N | -30.2 | -9.9 | -7.1 | -6.2 | -13.9 | -12.9 | -4.0 |
| Si-O-C-C | 56.1 | 31.2 | 27.8 | 26.7 | 36.3 | 34.7 | 16.7 |
| C-C-N-Si | 24.1 | 31.0 | 31.7 | 31.8 | 29.8 | 29.2 | 19.6 |
| O-C-C-N | -47.2 | -39.8 | -38.2 | -37.5 | -41.9 | -40.6 | -23.5 |
| q(Cl) | -0.372 | -0.420 | -0.495 | -0.546 | -0.389 | | |
| q(Si) | 1.565 | 1.720 | 1.754 | 1.771 | 1.717 | | |
| q(N) | -0.715 | -0.754 | -0.776 | -0.784 | -0.741 | | |
| q(O) | -0.733 | -0.775 | -0.776 | -0.781 | -0.764 | | |
| q(C-O) | 0.012 | -0.003 | -0.009 | -0.015 | 0.004 | | |
| q(C-N) | -0.134 | -0.170 | -0.180 | -0.186 | -0.163 | | |
| ρ _b (Si-N) | 0.185 | 0.297 | 0.379 | 0.426 | 0.245 | | |
| ∇ ² ρ _b (Si-N) | 1.231 | 2.330 | 3.984 | 5.013 | 1.514 | | |
| ρ _b (Cl-Si) | 0.661 | 0.651 | 0.609 | 0.564 | 0.694 | | |
| ∇ ² ρ _b (Cl-Si) | 6.474 | 5.935 | 5.555 | 4.920 | 7.019 | | |
| ρ _b (Si-O) | 0.902 | 0.869 | 0.863 | 0.864 | 0.879 | | |
| ∇ ² ρ _b (Si-O) | 26.062 | 24.575 | 24.139 | 24.076 | 25.219 | | |
| ρ _b (O-C) | 1.697 | 1.711 | 1.717 | 1.698 | 1.745 | | |
| ∇ ² ρ _b (O-C) | 0.038 | -0.149 | -0.504 | -0.431 | 0.039 | | |
| ρ _b (C-C) | 1.798 | 1.800 | 1.808 | 1.810 | 1.806 | | |
| ∇ ² ρ _b (C-C) | -17.878 | -17.940 | -18.086 | -18.116 | -18.034 | | |
| ρ _b (C-N) | 1.847 | 1.819 | 1.777 | 1.756 | 1.839 | | |
| ∇ ² ρ _b (C-N) | -19.631 | -18.120 | -16.963 | -16.242 | -18.760 | | |
| ΔE ⁽²⁾ n → R _y * (Si) | 7 | 20 | | 46 | | | |
| ΔE ⁽²⁾ n → s* (Si-Cl) | 24 | 55 | | 97 | | | |
| ΔE ⁽²⁾ n → s* (Si-O) | 18 | 48 | | 73 | | | |

^a Distances in Å, angles in degrees, Mulliken charges, q , in e, electron density at the BCP, ρ_b , in e Å⁻³, Laplacian of the electron density at the BCP, $\nabla^2\rho_b$, in e Å⁻⁵, donor-acceptor stabilization energy, $\Delta E^{(2)}$, in kJ mol⁻¹. ^b Experimental, C₃-symmetrized, crystal structure.

The results of the quantum mechanical calculations on the various clusters are summarized in Table 1. As is evident from this table, the effect of the neighboring molecules on the length of the Si-N distance is dramatic. Even in the smallest clusters **1**, the Si-N is 0.3 Å shorter than in the isolated molecule, adding another 0.1 Å to the shortening resulting from the steric effects calculated with the ONIOM method. This trend continues in **2** and **3**, where the calculated value comes very close to the experimental distance. As mentioned earlier, in terms of classical dipole-dipole interactions, these two models stabilize the central molecule even more than model **1**. Model **4**, however, demonstrates the large effect of the relative position of the surrounding molecules on the Si-N distance, with the value dropping essentially back to the one obtained with the ONIOM method. The Si-Cl bond undergoes the opposite, though less pronounced, transformation. The gas phase value of 2.058 Å increases gradually to 2.129 Å in **3**, in reasonable accordance with the experimental X-ray values. Note that the value obtained in **4** is actually shorter than in the isolated molecule. Changes in the other bonds are more subtle. An increase in length is also observed for the Si-O and C-N bonds. These are expected to be the most affected by a change in the nature of the dative bond. In addition to changes in the bond length, it is instructive to highlight a few changes in the valence angles. The Cl-Si-O

angle, for example, decreases from 104.4° in the gas phase to 94.5° in **3**, whereas O-Si-N changes from 76.0° to 84.5°. Both these observations indicate that the Si atom changes from a four-coordinated tetrahedron to a pentacoordinated bipyramid. However, not all valence angles change in the direction of a better correspondence with the experimental values. For example, both the O-C-C and C-C-N angles decrease in value whereas an increase would improve the situation. The torsion angles also change and the five-membered ring adopts a conformation somewhere between a twist and an envelop form. The isolated molecule **0** and cluster **1** were also calculated at the B3LYP/DFT level of theory. The Si-N length is found to decrease from 2.410 to 2.226 Å. The shorter bond calculated for the gas phase molecule is consistent with MP2 calculations reported earlier.^{15,17,18} Although details are different, the trends observed are the same as for the SCF calculations. More data are given in the Supporting Information.

Not unexpectedly, the changes in geometry and the interaction with the surrounding molecules result in a change of the charge distribution in the central molecule. The Mulliken charge on the chlorine atom becomes more negative from -0.372 to -0.546 e in **3**, a change of 47%. The silicon atom becomes more positive, increasing from 1.565 to 1.771 e (+17%). The overall change in the charge distribution is compatible with the

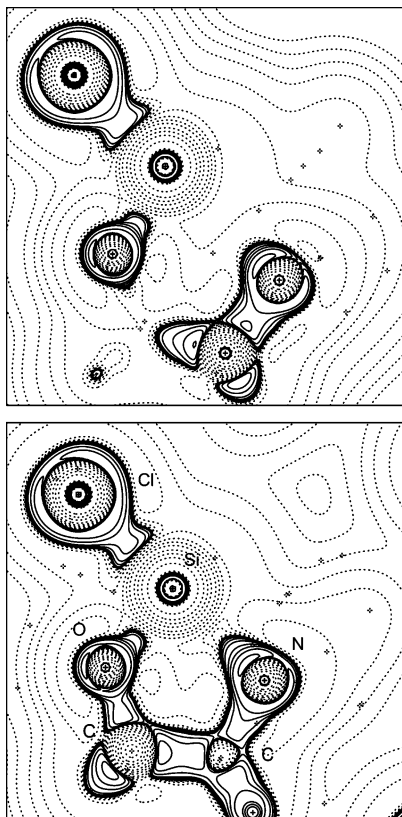


Figure 3. Laplacian, $\nabla^2\rho(\mathbf{r})$, of the electron density of chlorosilatrane in the gas phase (top), and model **3** in the crystalline state (bottom). Solid lines represent areas of local charge concentration; dotted lines, areas of charge depletion.

mental picture of negative charge being redistributed from the silicon and hydrogen atoms toward the other atoms in the molecule. The differences of the Si–N interaction between the gas phase and the crystal are also apparent in other properties of the electron distribution, $\rho(\mathbf{r})$. As mentioned by Gordon et al.,⁹ a bond critical point (BCP) can be found between the Si and N atoms, indicating the existence of a “bond”. Bond critical points between Si and N were found in all models, **0**–**4**. The second derivative, or Laplacian of $\rho(\mathbf{r})$, $\nabla^2\rho(\mathbf{r})$, gives information about a local increase or decrease of the electron distribution and also allows us to extract more information about the nature of a BCP.

Figure 3 shows a contour diagram of the Laplacian of the electron density of chlorosilatrane in the plane defined by the Si and N atoms, and one O atom, calculated for the isolated molecule, and for the cluster **3**. There are some striking differences between the two pictures. First there is the change in the conformation of the five-membered ring, making all the atoms more visible in the bottom picture. The interesting part, however, is the region between the N atom and silicon. Not only is the decrease in the Si–N distance very visible, it can also be seen clearly that there is a large increase in electron density in the transannular region toward the Si atom. Another noticeable aspect is the “thinner” area of electron density accumulation in the Si–Cl bonding region. These observations are reflected in the numerical values of $\rho_b(\mathbf{r})$ and $\nabla^2\rho_b(\mathbf{r})$, the electron density and its second derivative at the bond critical points, respectively. At the Si–N BCP, $\rho_b(\mathbf{r})$ goes from 0.185 e \AA^{-3} for the isolated molecule to 0.426 e \AA^{-3} in **3**, an increase of 130%. Even in cluster **4**, which in terms of dipole–dipole interactions destabilizes the central molecule, the value of 0.245 e \AA^{-3} is 33% higher than in the gas phase. The position of the

BCP moves with the N atom toward the silicon, both in absolute and in relative terms, and is situated at about 49% of the Si–N distance measured from Si in the isolated molecule, and 39% in model **3**. The Laplacian at the BCP is positive, which is typical for a nonsharing bond interaction. Its numerical value increases more than 4-fold between **0** and **3**, indicative of an increase in curvature in the electron density, but this is not surprising considering the shortening of the Si–N distance. For Si–Cl, $\rho_b(\mathbf{r})$ drops from 0.662 e \AA^{-3} in the gas phase to 0.564 e \AA^{-3} in **3**, consistent with the observed corresponding bond lengthening. A similar observation can be made for the Si–O bond, where the value changes from 0.902 to 0.864 e \AA^{-3} . The values of $\rho_b(\mathbf{r})$ for the other bonds are much higher and are typical for covalent bonds, e.g., 1.698 e \AA^{-3} in O–C, 1.810 e \AA^{-3} in C–C, and 1.756 e \AA^{-3} for C–N. Nevertheless, it is worthy to note that the electron density at the BCP between Si and N is similar to that for Si–Cl. A very recent determination of the deformation³⁶ electron density in crystalline methylsilatrane makes a comparison of these results with experiment possible. Lyssenko et al. confirm the existence of a BCP between Si and N and determine the electron density at this point to be 0.42 e \AA^{-3} , in excellent agreement with the value for the chloro compound calculated with cluster **3**. The value of 0.99 e \AA^{-3} for the Si–O bond is higher than found in this work but still within reasonable agreement, as are the values for the other bonds, e.g., 1.66 e \AA^{-3} for C–C, 1.79 e \AA^{-3} for C–O, and 1.73 e \AA^{-3} for C–N. The correspondence between the values of the Laplacian, $\nabla^2\rho_b(\mathbf{r})$, is not so good, but it is not clear what the significance is of this observation.

The chlorosilatrane molecule was also studied within the NBO framework.³³ The NBO atomic charges differ from the Mulliken charges, especially for silicon, but when the isolated molecule is compared with the crystal, the trend remains the same; i.e., the silicon becomes more positive and the chlorine atom more negative, as do the O- and N-atoms. The natural atomic orbitals (NAO) Wiberg bond index, which gives an indication of the bond order between two atoms, changes from 0.064 in **0** to 0.220 in **3** for Si–N and decreases from 0.795 to 0.675 for the Si–Cl bond, in line with the interpretation of the data calculated at the BCPs, suggesting an increase in bond strength between N and Si, and a weakening of the Si–Cl bond. The real usefulness of the NBO analysis is that it uses the electron density as a criterion to allow one to differentiate quantitatively between possible Lewis structures, and hence to investigate the existence of a bond between the Si and N atoms. For the gas phase, the Lewis structure with a lone pair in the N-atom, **b** in Chart 2, is calculated to have 0.723 non-Lewis valence electrons, whereas structure **c**, with a dative bond, has 0.832 electrons. Although this analysis thus favors a model with no Lewis bond, the numerical difference between the two structures is not very large. In addition, the NBO representing the dative bond in structure **c** is of the form $\Psi = 0.121\psi(\text{Si}) + 0.993\psi(\text{N})$, meaning that the nitrogen atom contributes more than 98% to the orbital, and hence that *quantitatively*, within the NBO framework, **c** is actually similar to, if not the same as **b**. In cluster **3**, the difference between the two models becomes insignificant, the amount of non-Lewis valence electrons being 0.792 e for **b** and 0.813 e for model **c**. On the other hand, the bond orbital becomes $\Psi = 0.232\psi(\text{Si}) + 0.973\psi(\text{N})$, still overwhelmingly dominated by nitrogen, but with its contribution dropping to 95%. Thus the Si–N “bond” is essentially the lone pair of the nitrogen interacting weakly with the silicon,³⁷ and more strongly so in the crystalline state. The relative high number of electrons that cannot be accommodated with either

Lewis structure, however, indicates that a delocalized model may be more appropriate for chlorosilatrane. A three center–four electron bond has been proposed before,^{38,39} but the NBO program did not confirm this as being viable. The NBO analysis also suggests that donation of the nitrogen lone pair to a suitable antibonding orbital will stabilize the molecule. As can be seen from Table 1, the major candidates are donation into an antibonding extra-valence orbital situated on the Si atom, and the antibonding σ_{SiCl}^* and σ_{SiO}^* orbitals. The latter two are compatible with the lengthening of these bonds in the series **0–3**.

The molecule was also studied in terms of natural resonance theory³⁵ (NRT), as explained in the computational details. Taking the value of the variational functional, $d(0)$, and the non-Lewis electron density as a criterion, the results show that a single reference NRT calculation is the most effective with **b** as a reference, followed closely by **c**. The Lewis structures **a** and **d** are considerably worse, and can be ignored. The multi-reference analysis rules out the combination **a+b** and **b+d**, and strongly favors **b+c**, assigning a 79:21% weight to the two Lewis structures. However, the NRT expansion with this combination as a reference, is only able to explain about 59% of the electron density, assigning the remainder to a large variety of additional resonance structures. Again, this finding implies that it is not easy to localize the electron density in this molecule using the Lewis electron pair concept.

The shorter Si–N bond length of chlorosilatrane in the gas phase compared to the crystal should translate itself in a higher wavenumber of the corresponding stretching mode. For example, a recent computational study²⁶ on BH_3NH_3 showed that the value of the B–N stretching frequency differs by about 200 cm^{-1} between the gas phase and the solid state. Although no experimental vibrational spectrum has been published for chlorosilatrane, data are available for a number of other 1-substituted silatranes.^{40,41} Imbenotte et al.⁴⁰ assigned the Si–N stretching frequency for a number of silatranes to peaks at around 350 cm^{-1} , except for the fluoro compound, which is found at 398 cm^{-1} . Ignat'ev et al.⁴¹ studied hydrosilatrane and a deuterated form of this molecule and determined with the aid of the determination of the force constants a peak at 468 cm^{-1} (25% Si–N) and another at 596 cm^{-1} (37% Si–N) to have a high Si–N stretching component. For the deuterated compound, the values are 440 (27%) and 537 cm^{-1} (28%), respectively. Not unexpectedly, the calculated Si–N stretching mode is highly coupled with other vibrational modes. For the isolated molecule, a mode at 201 cm^{-1} is a combination of a cage deformation and Si–N stretch, and another at 450 cm^{-1} is a Si–N/Si–Cl stretching combination. Because of the way the clusters are calculated, the spectrum of **1** contains a large number of imaginary wavenumbers, corresponding to normal modes of the fixed surrounding molecules. However, identification of the two normal modes mentioned above proved to be straightforward, and these were found at 201 and 465 cm^{-1} . These results suggest that the Si–N stretching frequency is influenced by the crystal environment, as expected, but that the change is considerably less than found for, e.g., BH_3NH_3 .²⁶ Assuming a linear dependency between the wavenumber and the bond length as found in the latter,²⁶ the value of 450 cm^{-1} would only increase to about 485 cm^{-1} for the experimental bond length of 2.023 Å in the crystal. After applying a scale factor of 0.9 as is common, the value obtained is 435 cm^{-1} . This is in reasonable agreement with one peak identified by Ignat'ev et al.⁴¹ for the parent hydrogen silatrane. However, in view of the limitations in accuracy of this two-point extrapolation, it is probably more

sensible to predict that the Si–N stretching frequency is somewhere in the region 350–500 cm^{-1} .

Conclusions

The ONIOM and full ab initio calculations show that the Si–N distance in crystalline chlorosilatrane shortens by about 25% compared to the gas phase as the result of a conformational change, with the remainder being due to dipole–dipole interactions. The progression observed for models **0–3** indicates that good computational results can be obtained with relatively small clusters if stabilizing dipole–dipole interactions dominate in the model. The results for **4** on the other hand demonstrate that very large clusters are needed if a more realistic computational model is required. Alternatively, the result may be an indication that the use of the Hartree–Fock level of theory is inadequate for this type of calculations.

Analysis of the electron density in terms of the theory of atoms in molecules is in good agreement with existing experimental data for methylsilatrane, and indicates a large increase in electron density in the transannular Si–N region, and a decrease in the strength of the Si–Cl bond. NBO analysis shows that the formal Lewis structures with or without a Si–N bond are numerically almost identical to the former, and that both fit the calculated electron density equally well. Departures from the idealized Lewis structure are highlighted by the relative large amount of “non-Lewis” electron density, and the high stabilization energy for several donor–acceptor interactions. This result is essentially confirmed by the NRT calculations.

A calculation of the vibration spectrum of chlorosilatrane could only be performed for cluster **1** and a smaller basis set. As a result, the Si–N stretching band can only be predicted to be in the broad region 350–500 cm^{-1} , in fair to reasonable agreement with existing experimental assignments performed for related silatranes.

Acknowledgment. I thank Dr. Catharine Esterhuysen and Mr. Gerhard Venter for stimulating discussions. This work was supported by the National Research Foundation, grant number 2053646.

Supporting Information Available: Final coordinates of all calculations, an extended version of Table 1, Laplacians of the electron density for all models **0–4**, and an animation showing the conformational flexibility of chlorosilatrane. This material is available free of charge via the Internet at <http://pubs.acs.org>

References and Notes

- (1) Voronkov, M. G. *Top. Curr. Chem.* **1979**, *84*, 77.
- (2) Verkade, J. G. *Coord. Chem. Rev.* **1994**, *137*, 233–295.
- (3) Allen, F. H. *Acta Crystallogr. Sect. B* **2002**, *58*, 380–388.
- (4) Shen, Q.; Hilderbrandt, R. L. *J. Mol. Struct.* **1980**, *64*, 257–262.
- (5) Parkanyi, L.; Bihatsi, L.; Hencsei, P. *Cryst. Struct. Commun.* **1978**, *7*, 435.
- (6) Forgács, G.; Kolonits, M.; Hargittai, I. *Struct. Chem.* **1990**, *1*, 245–250.
- (7) Párkányi, L.; Hencsei, P.; Bihátsi, L.; Müller, T. *J. Organomet. Chem.* **1984**, *269*, 1–9.
- (8) (a) Greenberg, A.; Wu, G. *Struct. Chem.* **1989**, *1*, 79–85. (b) Greenberg, A.; Plant, C.; Venanzi, C. A. *J. Mol. Struct. (THEOCHEM)* **1991**, *234*, 291–301.
- (9) Gordon, M. S.; Carroll, M. T.; Jensen, J. H.; Davis, L. P.; Burggraf, L. W.; Guidry, R. M. *Organometallics* **1991**, *10*, 2657–2660.
- (10) Bader, R. F. W. *Atoms in Molecules. A quantum theory*; Oxford University Press: Oxford, U.K., 1990.
- (11) Csonka, G. I.; Hencsei, P. *J. Organomet. Chem.* **1993**, *446*, 99.
- (12) Csonka, G. I.; Hencsei, P. *J. Mol. Struct. (THEOCHEM)* **1993**, *283*, 251–259.

- (13) Csonka, G. I.; Hencsei, P. *J. Organomet. Chem.* **1993**, 454, 15.
- (14) Csonka, G. I.; Hencsei, P. *J. Comput. Chem.* **1994**, 15, 385–394.
- (15) Boggs, J. E.; Peng, C.; Pestunovich, V. A.; Sidorkin, V. F. *J. Mol. Struct. (THEOCHEM)* **1995**, 357, 67–73.
- (16) Dahl, T.; Skancke, P. N. *Int. J. Quantum Chem.* **1996**, 60, 567–578.
- (17) Csonka, G. I.; Hencsei, P. *J. Mol. Struct. (THEOCHEM)* **1996**, 362, 199–208.
- (18) Csonka, G. I.; Hencsei, P. *J. Comput. Chem.* **1996**, 17, 767–780.
- (19) (a) Onsager, L. *J. Am. Chem. Soc.* **1936**, 58, 1486–1493. (b) Kirkwood, J. G. *J. Chem. Phys.* **1934**, 2, 351–361. (c) 150. Wong, M. W.; Frisch, M. J.; Wiberg, K. B. *J. Am. Chem. Soc.* **1991**, 113, 4776–4782. (d) Wong, M. W.; Wiberg, K. B.; Frisch, M. J. *J. Am. Chem. Soc.* **1992**, 114, 523–529. (e) Wong, M. W.; Wiberg, K. B.; Frisch, M. J. *J. Chem. Phys.* **1991**, 95, 8991–8998. (f) Wong, M. W.; Wiberg, K. B.; Frisch, M. J. *J. Am. Chem. Soc.* **1992**, 114, 1645–1652.
- (20) Chung, G.; Kwon, O.; Kwon, Y. *Inorg. Chem.* **1999**, 38, 197–200.
- (21) Reed, A. E.; Weinstock, R. B.; Weinhold, F. *J. Chem. Phys.* **1985**, 83, 735–746.
- (22) Anglada, J. M.; Bo, C.; Bofill, J. M.; Crehuet, R.; Poblet, J. M. *Organometallics* **1999**, 18, 5584–5593.
- (23) Haaland, A. *Angew. Chem., Int. Ed. Engl.* **1989**, 28, 992.
- (24) Bühl, M.; Steinke, T.; v.R. Schleyer, P.; Boese, R. *Angew. Chem., Int. Ed. Engl.* **1991**, 30, 1160–1161.
- (25) Jonas, V.; Frenking, G.; Reetz, M. T. *J. Am. Chem. Soc.* **1994**, 116, 8741–8753.
- (26) Dillen, J.; Verhoeven, P. *J. Phys. Chem. A* **2003**, 107, 2570–2577.
- (27) Frisch, M. J.; Trucks, G. W.; Schlegel, H. B.; Scuseria, G. E.; Robb, M. A.; Cheeseman, J. R.; Zakrzewski, V. G.; Montgomery, J. A.; Stratmann, R. E., Jr.; Burant, J. C.; Dapprich, S.; Millam, J. M.; Daniels, A. D.; Kudin, K. N.; Strain, M. C.; Farkas, O.; Tomasi, J.; Barone, V.; Cossi, M.; Cammi, R.; Mennucci, B.; Pomelli, C.; Adamo, C.; Clifford, S.; Ochterski, J.; Petersson, G. A.; Ayala, P. Y.; Cui, Q.; Morokuma, K.; Malick, D. K.; Rabuck, A. D.; Raghavachari, K.; Foresman, J. B.; Cioslowski, J.; Ortiz, J. V.; Baboul, A. G.; Stefanov, B. B.; Liu, G.; Liashenko, A.; Piskorz, P.; Komaromi, I.; Gomperts, R.; Martin, R. L.; Fox, D. J.; Keith, T.; Al-Laham, M. A.; Peng, C. Y.; Nanayakkara, A.; Gonzalez, C.; Challacombe, M.; Gill, P. M. W.; Johnson, B.; Chen, W.; Wong, M. W.; Andres, J. L.; Gonzalez, C.; Head-Gordon, M.; Replogle, E. S.; Pople, J. A., *Gaussian 98, Revision A.7*. Gaussian, Inc., Pittsburgh, PA, 1998.
- (28) Kemme, A. A.; Bleidelis, Ya. Ya.; Pestunovich, V. A.; Baryshok, V. P.; Voronkov, M. G. *Dokl. Akad. Nauk SSSR* **1978**, 243, 688–691.
- (29) Rappé, A. K.; Casewit, C. J.; Colwell, K. S.; Goddard, W. A., III; Skiff, W. M. *J. Am. Chem. Soc.* **1992**, 114, 10024–10035.
- (30) Molecular Simulations Inc. *Cerius²* release 3.8, San Diego, CA, 1998.
- (31) Dillen, J. *QCPE Bull.* **1993**, 13, 6.
- (32) (a) Svensson, M.; Humbel, S.; Froese, R. D. J.; Matsubara, T.; Sieber, S.; Morokuma, K. *J. Phys. Chem.* **1996**, 100, 19357–19363. (b) Dapprich, S.; Komáromi, I.; Byun, K. S.; Morokuma, K.; Frisch, M. J. *J. Mol. Struct. (THEOCHEM)* **1999**, 461–462, 1–21.
- (33) FASTER, J. P.; Weinhold, F. *J. Am. Chem. Soc.* **1980**, 102, 7211–7218.
- (34) Glendening, E. D.; Badenhop, J. K.; Reed, A. E.; Carpenter, J. E.; Bohmann, J. A.; Morales, C. M.; Weinhold, F. *NBO 5.0*; Theoretical Chemistry Institute, University of Wisconsin, Madison, WI, 2001.
- (35) (a) Glendening, E. D.; Weinhold, F. *J. Comput. Chem.* **1998**, 19, 593–609. (b) Glendening, E. D.; Weinhold, F. *J. Comput. Chem.* **1998**, 19, 610–627. (c) Glendening, E. D.; Badenhop, J. K.; Weinhold, F. *J. Comput. Chem.* **1998**, 19, 628–646.
- (36) Lyssenko, K. A.; Korlyukov, A. A.; Antipin, M. Yu.; Knyazev, S. P.; Kirin, V. N.; Alexeev, N. V.; Chernyshev, E. A. *Mendeleev Commun.* **2000**, 10, 88–90.
- (37) Schmidt, M. W.; Windus, T. L.; Gordon, M. S. *J. Am. Chem. Soc.* **1995**, 117, 7480–7486.
- (38) Schklover, V. E.; Struchkov, Yu. T.; Voronkov, M. G. *Russ. Chem. Rev.* **1989**, 58, 211.
- (39) Sidorkin, V. F.; Pestunovich, V. A.; Voronkov, M. G. *Dokl. Akad. Nauk SSSR* **1977**, 235.
- (40) Imbenotte, M.; Palavit, G.; Legrand, P. *J. Raman Spectrosc.* **1983**, 14, 135–137.
- (41) Ignat'ev, I. S.; Lazarev, A. N.; Shevchenko, S. G.; Baryshok, V. P. *Izvest. Akad. Nauk SSSR, Ser. Khim.* **1986**, 7, 1518–1526.